e-ISSN : 2987-0836 DOI: https://doi.org/10.59585/ijhs

Publish : Association of Indonesian Teachers and Lecturers
International Journal of Health Sciences (IJHS)
Journal Homepage : https://jurnal.agdosi.com/index.php/IJHS/index
Volume 4 | Number 4 | December 2026 |

Thermal Barrier Coatings (TBC) For Carbon Fiber-Reinforced Polymer (CFRP) Composites: A Review

Fesa Mahardika Anastasya*, Sovian Aritonang, Hotma Renta R. Siringoringo, Richard Panjaitan, Cindy Florecita, Luthfiah Maharani

*Faculty of Military Mathematics and Natural Sciences, Indonesia Defense University, Indonesia

Abstract

Carbon fiber-reinforced polymer (CFRP) composites are widely used in high-performance lightweight structures, yet their thermoset matrices begin to decompose at about 300°C, which limits their use in high-temperature environments. This article presents a comparative narrative review of two studies on thermal barrier coatings (TBCs) for CFRP developed by the same research group. The first study used a compression-molded Al_2O_3 plate mechanically bonded to CFRP through vacuum-assisted resin transfer molding (VARTM), whereas the second used a double-layered yttria-stabilized zirconia (YSZ) TBC with graded porosity produced by flame spraying with PEEK particles as a pore former. Fabrication parameters, microstructure, thermal conductivity, thermal shock response, and residual flexural performance were extracted from both studies and compared. In the first study, a 1.45 mm TBC reduced the back-surface temperature of CFRP to 188–228°C under 500–700°C flames while retaining 90%, 62%, and 50% of the failure load, whereas uncoated CFRP lost 93–95% at 600–700°C. In the second study, a TBC about 0.66 mm thick with a thermal conductivity of about 0.3 W/m·K held the back surface at 230°C for 10 minutes under a 500°C flame, retaining 87% of flexural strength and 75% of modulus, while uncoated CFRP ignited. Both approaches are effective but rely on different protection mechanisms. Non-uniform test protocols, the absence of areal mass data, and the lack of long-term cyclic testing are the main limitations to be addressed in future work.

Keywords: thermal barrier coating, CFRP, thermal conductivity, thermal shock, porosity

Correspondent Author : Fesa Mahardika Anastasya
E-mail : fesamahardikaanastasya@gmail.com

International Journal of Health Sciences is licensed under a Creative Commons Attribution 4.0 International License

e-ISSN : 2987-0836 DOI: https://doi.org/10.59585/ijhs

Publish : Association of Indonesian Teachers and Lecturers
International Journal of Health Sciences (IJHS)
Journal Homepage : https://jurnal.agdosi.com/index.php/IJHS/index
Volume 4 | Number 4 | December 2026 |

1. Introduction

Carbon fiber-reinforced polymer (CFRP) composites are widely used in aerospace, automotive, and energy applications because of their high strength-to-weight and stiffness-to-weight ratios (Kim et al., 2021; Kim et al., 2024). Their weak point under fire or other high-temperature exposure is the polymer matrix rather than the fibers. Common thermoset matrices such as epoxy, bismaleimide, and vinyl ester are flammable and begin to decompose at about 300–330°C (Kodur, Bhatt and Naser, 2019; Nguyen, Vu and Ferrier, 2019), whereas carbon fibers remain stable up to their sublimation temperature of roughly 3,316°C. One of the studies reviewed here recounts the Airbus A350 accident at Haneda airport, in which the CFRP fuselage delayed the spread of flame and heat into the cabin for up to 90 seconds but the aircraft ultimately burned completely (Kim et al., 2024). Fire-fighting drones are a typical example: they are used for disaster response (Ando et al., 2018; Restas, 2015), their lightweight frames benefit from fiber-reinforced composites (Kim et al., 2020), and their skins may face design-fire temperatures of several hundred degrees (Ariyanayagam and Mahendran, 2014). To keep the matrix below its decomposition temperature, active solutions such as thermoelectric cooling or cooling fans have been used, at the cost of added weight and complexity (Kim et al., 2021).

Thermal barrier coatings (TBCs) offer a passive alternative. A TBC is a low-conductivity, high-melting-point ceramic layer that sustains a steep temperature gradient through its thickness, so that the underlying material stays below its damage temperature (Padture, Gell and Jordan, 2002; Zhu and Miller, 2000). Alumina (Al_2O_3), yttria-stabilized zirconia (YSZ), and mullite are the most widely used TBC materials (Clarke and Phillpot, 2005; Vaßen et al., 2010; Lee et al., 2003). Comprehensive reviews of TBC materials, durability mechanisms, and processing are available (Clarke and Levi, 2003; Evans et al., 2001; Liu et al., 2019; Mehta et al., 2022), and newer concepts such as high-entropy oxides (Yao, Yang and Zhao, 2022) and multilayer systems (Leng, Romero and Hussain, 2023) continue to emerge. Conventional TBC manufacturing, namely thermal spraying (Tejero-Martin et al., 2019; Mittal and Paul, 2022; Fan and Bai, 2016) and vapor deposition (Altaf, Rahman and Wani, 2025), is carried out on metallic substrates at roughly 800–1,000°C (Feuerstein et al., 2008), temperatures that would destroy a polymer composite. Recent work on metallic substrates includes plasma-sprayed coatings on additively manufactured superalloys (Bellippady et al., 2024) and thick columnar coatings produced by suspension plasma spray (Chen and Dambra, 2024), while cold spray is a lower-temperature alternative (Guo et al., 2022; Dai et al., 2024). The thermal endurance of coatings on metals has been examined through thermal shock, thermal cycling, and hot corrosion tests (Ahmadi et al., 2019; Chen et al., 2011; Soleimanipour et al., 2016; Zhou et al., 2024). TBCs for CFRP have therefore received comparatively little attention and require different manufacturing strategies.

Earlier attempts to protect fiber-reinforced polymers include ceramic particles in epoxy or phenolic coatings (Luangtriratana, Kandola and Myler, 2015), nanoscale aluminum trihydroxide as a flame retardant in epoxy (Könnicke et al., 2011), alumina fiber mats (Golewski and Sadowski, 2018; Golewski and Sadowski, 2019), aerogel/epoxy coatings (Krishnaswamy et al., 2019), graphene nanoplatelet films (Cilento et al., 2023),

International Journal of Health Sciences is licensed under a Creative Commons Attribution 4.0 International License

e-ISSN : 2987-0836 DOI: https://doi.org/10.59585/ijhs

Publish : Association of Indonesian Teachers and Lecturers
International Journal of Health Sciences (IJHS)
Journal Homepage : https://jurnal.agdosi.com/index.php/IJHS/index
Volume 4 | Number 4 | December 2026 |

carbon nanotube–ceramic hybrid layers (Ju et al., 2018), and paint coatings (Jarrah et al., 2018; Khaneghahi et al., 2018). Most of these rely on an organic binder or matrix that burns out at high temperature, or require thick layers, or show weak adhesion or delamination (see Table 3).

Two recent studies from the Korea Institute of Science and Technology and Utah State University propose inorganic, ceramic-based TBCs that are integrated with CFRP through a standard vacuum-assisted resin transfer molding (VARTM) process. The first (Kim et al., 2021) uses a compression-molded Al_2O_3 plate; the second (Kim et al., 2024) uses a flame-sprayed, double-layered YSZ coating with tunable porosity. The same group has since extended the concept to atmospheric plasma-sprayed yttrium aluminum garnet coatings on carbon fabric (Praveen et al., 2026). Because the second study builds directly on the first and uses the same thermal shock concept, the two provide an unusually clean basis for comparison. This review (i) summarizes how each TBC is made and what microstructure results, (ii) compares their thermal and residual mechanical performance, and (iii) identifies limitations and research gaps for TBC-protected CFRP.

2. Research Methods

This article is a comparative narrative review of two primary studies: Kim et al. (2021) and Kim et al. (2024). They were selected because both address a TBC for CFRP, both integrate the coating by VARTM, and both evaluate it with a methane-burner thermal shock test followed by three-point bending, with the second study explicitly referring to the first for its test configuration.

For each study the following information was extracted: materials and fabrication route, microstructure (porosity, pore size, layer thickness), thermal conductivity, thermal shock conditions and back-surface temperatures, damage observations, residual flexural properties, and adhesion strength. Numerical values are quoted as reported by the original authors. Derived quantities, such as temperature reductions and percentage retention, were calculated from reported values and are identified as such. Additional literature cited in the two studies was used only to place their results in context (Table 3).

The approach has clear limits. Only two sources are included and both originate from the same group, there is no independent replication, and the review is not a systematic one. The figures in this article were redrawn by the authors from numerical values given in the source texts and are not reproductions of the original figures.

3. Research Results and Discussion

a. Research result

The two TBC systems differ in material, manufacturing route, and bonding mechanism, as summarized in Table 1. Their thermal and mechanical results are then compared in Tables 2 and 3 and Figures 1 to 3.

Fabrication routes and microstructure. The first study prepared a free-standing plate by hand-mixing α-phase Al_2O_3 powder (99.5% purity, mean particle diameter 9.27 μm) with a potassium-silicate ceramic binder at a 3.3:1 weight ratio, then curing the mixture in a mold at 96°C, 175°C, and 275°C (1 h each) under 300 kPa. The 1.45 mm plate was placed on 12 plies of plain-woven T300 carbon fabric and the assembly was infused with epoxy by VARTM. Evaporation of binder water leaves an open-pore network (void fraction

International Journal of Health Sciences is licensed under a Creative Commons Attribution 4.0 International License

e-ISSN : 2987-0836 DOI: https://doi.org/10.59585/ijhs

Publish : Association of Indonesian Teachers and Lecturers
International Journal of Health Sciences (IJHS)
Journal Homepage : https://jurnal.agdosi.com/index.php/IJHS/index
Volume 4 | Number 4 | December 2026 |

25.6%, mean void size 5.83 µm, density 1.93 g/cm^3). During infusion this network fills with resin, forming a branched interlocking structure; the measured lap shear strength was 6.56 ± 0.35 MPa (Kim et al., 2021).

The second study instead sprayed YSZ directly onto dry carbon fabric with an oxy-acetylene flame. The fabric was first desized in an acetone bath, which spreads the fibers within each tow and closes the openings at warp–weft intersections; without this step, holes of about 480 × 568 µm remained even after coating. A dense YSZ layer (about 207 µm, four passes) was sprayed first, followed by a porous layer co-sprayed with PEEK particles (six passes). Heat treatment at 500°C for 5 h burned the PEEK out and left pores. The coated fabric was then co-cured on a partially cured 12-ply laminate (80°C for 30 min, then 80°C for 3.5 h). Porosity was tuned through the PEEK injection distance D (2, 5, 8 cm) and feed rate R (0.8, 1.0, 1.3 g/min). Porosity rose with R (19%, 24%, 33%) and was lowest at D = 2 cm (17%) because most PEEK burned in the hotter flame, while at D = 8 cm (above 32%) a cooler flame left poorly melted, poorly bonded particles. Such sensitivity of coating microstructure to spray parameters is well known in thermal spraying (Xie et al., 2004). R = 1.3 g/min gave a 41% open-pore fraction but a fragile layer under vacuum, so D = 5 cm and R = 1.0 g/min were selected (about 24% porosity by image analysis and 31.6% open pores by the Archimedes method), adding about 0.66 mm to the laminate (Kim et al., 2024).

Table 1. Comparison of the two thermal barrier coating (TBC) systems for CFRP

Item	Study 1 (Kim et al., 2021)	Study 2 (Kim et al., 2024)
Ceramic phase	α-Al_2O_3 (9.27 µm) with potassium-silicate binder	7–8 wt% YSZ (≈25 µm spheres) with sacrificial PEEK (9–135 µm)
TBC forming route	Compression molding of powder–binder mixture (300 kPa; 96/175/275°C)	Oxy-acetylene flame spraying on desized dry carbon fabric; PEEK burn-out at 500°C, 5 h
Substrate and matrix	12-ply T300 3K plain weave; epoxy YDPN-638 with Jeffamine D230; VARTM, cured at 120°C (1 h) and 150°C (3 h)	12-ply T300 3K plain weave; epoxy YD 128 with BGE diluent and polyamide G-640; VARTM, 80°C (30 min) then 80°C (3.5 h)
Bonding mechanism	Resin penetrates open pores of pre-formed plate (mechanical interlocking)	Dense YSZ layer sprayed onto fiber tows; dense layer blocks resin up-flow
Added thickness	1.45 mm	≈0.66 mm
Porosity	25.6% (void fraction, X-ray microscopy)	≈24% (image analysis); 31.6% open pores (Archimedes)
Thermal conductivity, 25°C	3.38 W/m·K (without epoxy); 4.31 W/m·K (with epoxy)	≈0.3 W/m·K (double layer); 1.39 W/m·K (dense layer)
Adhesion strength	6.56 ± 0.35 MPa (single-lap shear)	5.45 ± 0.5 MPa (tensile adhesion)
Highest test temperature	700°C	500°C

Source: compiled by the authors from Kim et al. (2021) and Kim et al. (2024).

Thermal conductivity. In the first study the Al_2O_3 plate without epoxy had a conductivity of 3.38 W/m·K at 25°C, rising slightly to 3.94 W/m·K at 500°C, which the authors attribute to gas–solid contact and radiation in the porous structure (He and Xie, 2015). With epoxy filling the pores the value was 4.31 W/m·K, because epoxy (0.166–0.247 W/m·K) conducts better than air; this is 5.7–7.3 times the conductivity of neat CFRP

International Journal of Health Sciences is licensed under a Creative Commons Attribution 4.0 International License

e-ISSN : 2987-0836 DOI: https://doi.org/10.59585/ijhs

Publish : Association of Indonesian Teachers and Lecturers
International Journal of Health Sciences (IJHS)
Journal Homepage : https://jurnal.agdosi.com/index.php/IJHS/index
Volume 4 | Number 4 | December 2026 |

(0.59 W/m·K), a value in line with reported through-thickness conductivities of carbon/epoxy laminates (Tian and Cole, 2012; Fang et al., 2019; Yu, Wu and Feng, 2015; Bard et al., 2019; Kandare et al., 2015). In the second study the porous YSZ layer had a room-temperature conductivity of 0.54 to 0.44 W/m·K as R increased from 0.8 to 1.3 g/min, and conductivity decreased as D and R increased. The dense YSZ layer measured 1.06–1.39 W/m·K between 25°C and 400°C, and the double-layered TBC stayed nearly constant at about 0.3 W/m·K, against about 0.55 W/m·K for neat CFRP (Figure 1). The authors link this low value to splat boundaries and unmelted particles that scatter phonons, but did not test that explanation directly. The source reports 0.27 W/m·K in its abstract and 0.32 W/m·K in the main text.

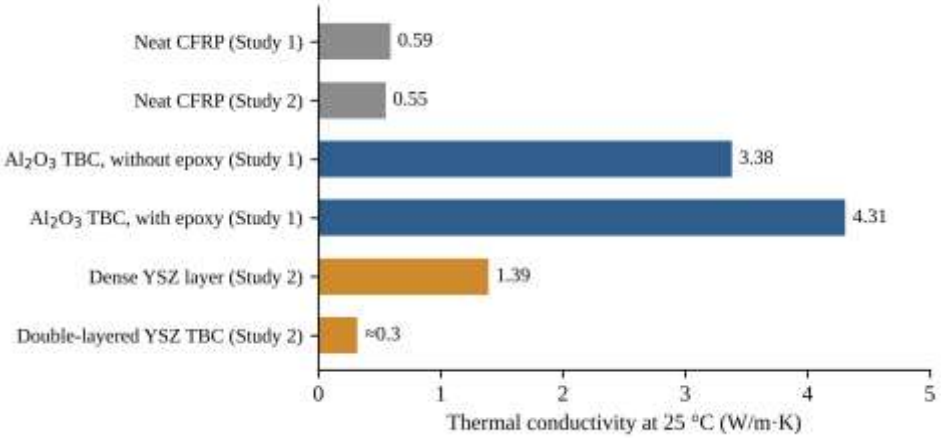


Figure 1. *Thermal conductivity of the CFRP substrates and TBC layers reported in the two studies at 25°C. Values for the double-layered YSZ TBC are approximate (0.27–0.32 W/m·K).*

Thermal shock response. Both studies used a methane burner for 10 min and controlled the hot-side temperature T_H through the burner–specimen distance. Study 1 tested T_H = 500, 600, and 700°C, whereas Study 2 tested 500°C. Table 2 lists the back-surface temperatures. In Study 1 the benefit of the coating grew with flame temperature: the reduction in T_{CFRP} was about 11°C at 500°C but 167°C and 298°C at 600°C and 700°C, and the coated substrate stayed below the roughly 300°C decomposition onset of epoxy in every case. In Study 2, the uncoated laminate reached 300°C after about 300 s and ignited, whereas the coated laminate held 230°C for the full 10 min without ignition (Figure 2).

Table 2. Back-surface temperature (T_{CFRP}) of neat and TBC-coated CFRP under flame exposure

Study	T_H (°C)	Neat CFRP, T_{CFRP} (°C)	TBC/CFRP, T_{CFRP} (°C)	Reduction (°C)	$R_{contact}$ (m^2·K/W)
1	500	199	188	11	0.06942
1	600	377	211	167	0.07685
1	700	526	228	298	0.08590
2	500	≥300 (ignited at ≈300 s)	230	n/a	not analyzed

Source: Kim et al. (2021) and Kim et al. (2024). $R_{contact}$ is the fitted interfacial thermal contact resistance from the one-dimensional resistance model of Study 1.

International Journal of Health Sciences is licensed under a Creative Commons Attribution 4.0 International License

e-ISSN : 2987-0836 DOI: https://doi.org/10.59585/ijhs

Publish : Association of Indonesian Teachers and Lecturers
International Journal of Health Sciences (IJHS)
Journal Homepage : https://jurnal.agdosi.com/index.php/IJHS/index
Volume 4 | Number 4 | December 2026 |

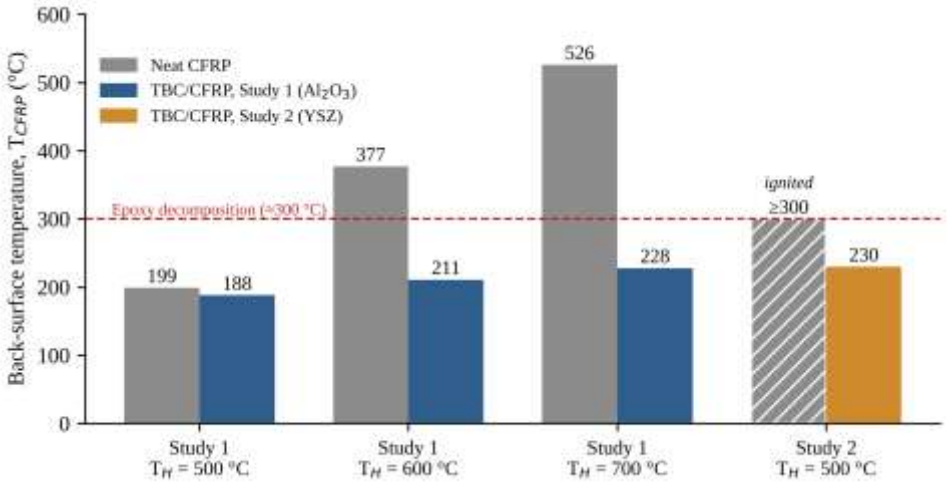


Figure 2. *Back-surface temperature of neat CFRP and TBC/CFRP in the thermal shock tests of Study 1 (Al_2O_3 TBC) and Study 2 (YSZ TBC). The Study 2 neat CFRP bar marks the temperature at which ignition began.*

The visible damage also differed. In Study 1 the Al_2O_3 TBC showed only discoloration at 500°C, scorching and micropores at 600°C, and through-thickness cracking and delamination at 700°C, attributed to the mismatch between the thermal expansion of alumina (7–8 × 10^{-6}/K; Hirata et al., 2016) and CFRP (1.33–29.0 × 10^{-6}/K; Dong et al., 2018); weight loss was at most 1.25 wt%. In Study 2 the coated specimen had no physical damage beyond surface scorching from residual PEEK, while the uncoated laminate delaminated severely. To explain the large temperature drop in Study 1, the authors fitted a one-dimensional thermal resistance circuit and obtained interfacial contact resistances of 0.06942, 0.07685, and 0.08590 $m^2 \cdot K/W$ at 500, 600, and 700°C, an increase of about 24% (calculated from the reported values). They interpret this as an air gap forming at the interface as the epoxy decomposes, and note that the one-dimensional assumption may overestimate it.

Residual mechanical performance. In Study 1 the failure load in three-point bending fell from 903 N for the pristine TBC/CFRP to 809 N (−10%), 557 N (−38%), and 453 N (−50%) after exposure at 500, 600, and 700°C, while the loss for uncoated CFRP at 600–700°C was 93–95%. A kink in the pristine stress–strain curve, caused by TBC fracture, disappeared after exposure because the epoxy in the TBC had decomposed. The ceramic–CFRP bond stayed intact even where the TBC cracked into two pieces. In Study 2 the flexural strength of TBC/CFRP decreased from 348 MPa to 302 MPa (−13%) and the modulus by 25% after exposure at 500°C. Uncoated CFRP could not be tested after exposure because it had burned, but its unexposed strength and modulus were 512 MPa and 29 GPa, so the unexposed coated laminate was about 32% weaker in flexure (calculated), which the authors attribute to the thickness and brittleness of the ceramic layer (Figure 3). The kink in the Study 2 curves marks delamination between the desized fabric carrying the YSZ coating and the underlying laminate: desized fibers have a non-polar surface and the partially cured epoxy was viscous, which weakened that interface, and tensile adhesion

International Journal of Health Sciences is licensed under a Creative Commons Attribution 4.0 International License

e-ISSN : 2987-0836 DOI: https://doi.org/10.59585/ijhs

Publish : Association of Indonesian Teachers and Lecturers
International Journal of Health Sciences (IJHS)
Journal Homepage : https://jurnal.agdosi.com/index.php/IJHS/index
Volume 4 | Number 4 | December 2026 |

failures occurred mainly at the first CFRP ply rather than in the ceramic. The authors ascribe the modulus loss to oxygen vacancies in YSZ at high temperature, an explanation that was not verified experimentally.

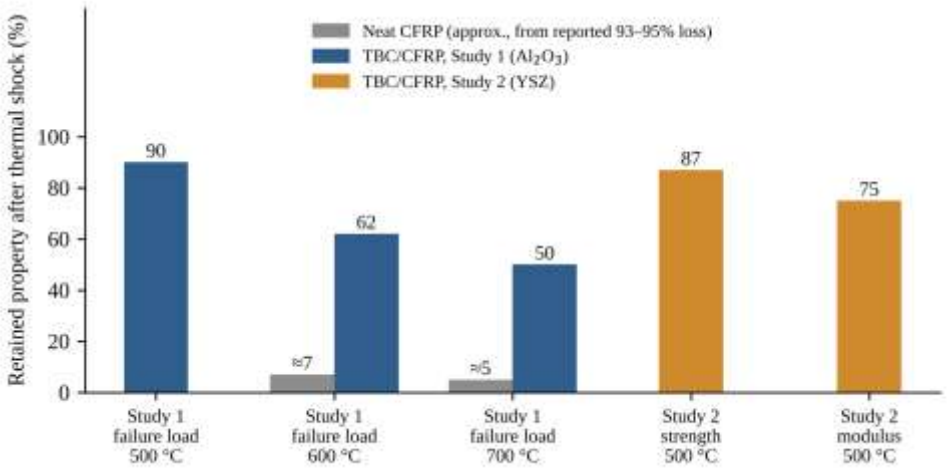


Figure 3. *Retained mechanical properties after thermal shock, calculated from the values reported in the two studies. Neat CFRP values are approximate and derived from the reported 93–95% loss at 600–700°C; no value is plotted for neat CFRP in Study 1 at 500°C or in Study 2, where the specimen burned.*

b. Discussion

The two coatings protect CFRP by different mechanisms. The Study 1 TBC is not a low-conductivity insulator: its conductivity (3.4–4.3 W/m·K) is several times that of the CFRP it protects, and the thermal resistance computed from that conductivity and a 1.45 mm thickness is small compared with the fitted contact resistance. The resistance model therefore assigns most of the temperature drop to an interfacial gap that forms as the epoxy decomposes. Localized heating and lateral heat spreading in the ceramic plate may also contribute, but this was not tested in either study. By contrast, Study 2 relies on intrinsic insulation: a thin, porous YSZ layer of about 0.3 W/m·K, with the interface remaining intact after exposure at 500°C. The first system therefore performs best at 600–700°C, where an interfacial gap develops, while the second delivers consistent protection at 500°C without relying on interfacial damage, although it was not tested at higher temperatures.

Absolute values from the two studies should not be compared directly. At T_H = 500°C the uncoated CFRP in Study 1 reached about 199°C, yet the uncoated CFRP in Study 2 passed 300°C and ignited. Plausible reasons are differences in epoxy system (YDPN-638/Jeffamine D230 versus YD 128/polyamide G-640), laminate thickness (2.4 mm versus 2.98 mm), temperature measurement (thermocouple and IR thermometer with set emissivities versus an IR camera), and burner settings, but the studies do not resolve this. In addition, the abstract of Study 2 quotes a porosity of 34% and conductivity of 0.27 W/m·K, whereas its main text and figures give about 24% and 0.32 W/m·K; this review follows the main text.

International Journal of Health Sciences is licensed under a Creative Commons Attribution 4.0 International License

e-ISSN : 2987-0836 DOI: https://doi.org/10.59585/ijhs

Publish : Association of Indonesian Teachers and Lecturers
International Journal of Health Sciences (IJHS)
Journal Homepage : https://jurnal.agdosi.com/index.php/IJHS/index
Volume 4 | Number 4 | December 2026 |

Each system also trades protection against strength or interface quality. The Study 1 TBC retained half of its failure load at 700°C, but with through-thickness cracks and delamination, consistent with thermal-gradient and expansion-mismatch delamination mechanisms described for TBCs (Hutchinson and Evans, 2002). Coating thickness and roughness are known to influence thermo-mechanical stress in TBC systems (Moridi, Azadi and Farrahi, 2014), and stress evolution has been modeled in detail for metallic substrates (Wang et al., 2022). On metals, failure under thermal gradients and cyclic loading (Liu et al., 2024) and degradation by CMAS deposits (Peng et al., 2012; Craig et al., 2015; Nieto et al., 2021) are well documented; whether comparable mechanisms matter for coatings on polymer composites has not been examined. The Study 2 TBC retained 87% of strength and 75% of modulus at 500°C, but the unexposed coated laminate was already weaker than the neat laminate, and its weakest link is the desized-fabric interface. Plausible improvements, which neither study demonstrates, include surface activation of the desized fibers, better control of resin viscosity during infusion, and tuning the thickness of the ceramic layer.

Table 3. Other thermal protection approaches for fiber-reinforced polymers reported in the literature

Approach	Reported performance	Main limitation reported
Ceramic particles in epoxy or phenolic coating (Luangtriratana, Kandola and Myler, 2015)	Time for the back surface of glass-fiber laminates to reach 180°C and 250°C increased by 49 s and 63 s at 35 kW/m^2 with sieved Al_2TiO_5	Organic binder decomposes at high temperature, releasing the ceramic particles
Alumina fiber mat with epoxy binder (Golewski and Sadowski, 2018)	5 mm layer reduced the back surface of CFRP to 150°C at 800°C for 1 min	Thick layer; damage from decomposition of the epoxy binder
Aerogel/epoxy dip coating (Krishnaswamy et al., 2019)	700 µm layer reduced the back-surface temperature by about 50°C at 100°C	Demonstrated at low temperature only
Graphene nanoplatelet film (Cilento et al., 2023)	62 µm film: surface about 520°C reduced to about 220°C behind 1.7 mm CFRP at 100 kW/m^2	Coating swelling and CFRP delamination
CNT–ceramic hybrid layer by polymer infiltration and pyrolysis (Ju et al., 2018)	Good structural integrity and high-temperature tolerance	About 24% weight loss above 610°C; costly, size-limited process
Intumescent paint (Khaneghahi et al., 2018)	Swells and blocks oxygen within about 350–600°C	Tensile strength of coated FRP bars fell 39.1% at 500°C and 64.2% at 700°C

Source: as reported in Kim et al. (2021) and Kim et al. (2024) for the studies cited. Test conditions differ among studies, so values are not directly comparable.

Compared with these approaches, the two reviewed TBCs avoid organic binders in the protective layer and are comparatively thin: 1.45 mm and about 0.66 mm, against 5 mm for the alumina fiber mat, although that mat was tested under a different heat load and duration. Their intended applications are fire-fighting drones, battery housings, and wildfire exposure, where flame or smoke temperatures of roughly 420–600°C are relevant

International Journal of Health Sciences is licensed under a Creative Commons Attribution 4.0 International License

e-ISSN : 2987-0836 DOI: https://doi.org/10.59585/ijhs

Publish : Association of Indonesian Teachers and Lecturers
International Journal of Health Sciences (IJHS)
Journal Homepage : https://jurnal.agdosi.com/index.php/IJHS/index
Volume 4 | Number 4 | December 2026 |

(Dennison et al., 2006; Morvan and Dupuy, 2004). Study 2 also argues that flame spraying is portable and suited to large areas, but cost and processing time were not quantified. Alumina-based ceramics are also being developed by laser-directed energy deposition with attractive thermal properties (Zhao et al., 2024; Zhao et al., 2025), which could in principle offer alternative routes to alumina layers, although process temperatures would need to be compatible with polymer substrates.

Several gaps remain. Neither study reports the areal mass added by the TBC, an essential figure for lightweight structures. Exposure was one-sided, for 10 min, and without thermal cycling, impact, erosion, or long-term aging. The heat flux of the burner was not quantified, the temperature of the TBC surface rests on assumed emissivities, and neither study includes independent replication. Future work should apply one standardized thermal shock protocol to both coating types, report mass-normalized thermal and mechanical metrics, extend testing to cyclic and higher-flux exposure, and examine whether the interlocking of Study 1 and the low conductivity of Study 2 can be combined. Data-driven models trained on spray parameters (Zhu et al., 2023; Alkurdi et al., 2024) and terahertz non-destructive measurement of porosity (Ye et al., 2024) could also support the porosity and property tuning that Study 2 performed experimentally.

4. Conclusion

Based on the comparative review of the two studies on thermal barrier coatings for CFRP, it can be concluded as follows:

a. Both the compression-molded Al_2O_3 TBC (1.45 mm) and the flame-sprayed double-layered YSZ TBC (about 0.66 mm) kept the CFRP back surface below the roughly 300°C decomposition onset of epoxy, at 188–228°C under 500–700°C flames and at 230°C under a 500°C flame, respectively, while uncoated CFRP was severely damaged or ignited.

b. The protection mechanisms differ. The Al_2O_3 TBC has a conductivity of 3.4–4.3 W/m·K, and its large temperature drop at 600–700°C is attributed to an interfacial air gap, whereas the YSZ TBC depends on intrinsic low conductivity (about 0.3 W/m·K) controlled by PEEK injection distance and feed rate.

c. Residual flexural performance was 50–90% for the Al_2O_3 TBC (500–700°C) and 87% of strength and 75% of modulus for the YSZ TBC (500°C), compared with a 93–95% loss for uncoated CFRP in the first study. Non-uniform test protocols, missing mass data, and the lack of cyclic and long-term tests limit direct comparison and practical qualification.

5. Compliance with ethical standards Acknowledgements

The authors thank the original authors of the two studies reviewed here for the data on which this article is based, and Republic of Indonesia Defense University for institutional support.

Disclosure of conflict of interest

The authors declare that they have no conflict of interest.

International Journal of Health Sciences is licensed under a Creative Commons Attribution 4.0 International License

e-ISSN : 2987-0836 DOI: https://doi.org/10.59585/ijhs

Publish : Association of Indonesian Teachers and Lecturers
International Journal of Health Sciences (IJHS)
Journal Homepage : https://jurnal.agdosi.com/index.php/IJHS/index
Volume 4 | Number 4 | December 2026 |



Statement of informed consent

Not applicable. This article is a literature-based review and involved no human participants or animals.

References

Ahmadi, M. S., Shoja-Razavi, R., Valefi, Z. and Jamali, H. (2019) 'The effect of laser surface treatment on the thermal shock behavior of plasma sprayed Al_2O_3/YSZ multilayer thermal barrier coatings', *Surface and Coatings Technology*, 366, pp. 62–69. doi: 10.1016/j.surfcoat.2019.03.024.

Alkurdi, A. A. et al. (2024) 'Enhancing mechanical behavior assessment in porous thermal barrier coatings using a machine learning fine-tuned with genetic algorithm', *Journal of Thermal Spray Technology*, 33(4), pp. 824–838. doi: 10.1007/s11666-024-01756-w.

Altaf, S. F., Rahman, A. and Wani, M. (2025) 'Long-term stability and performance of nanostructured thermal barrier coatings deposited by magnetron sputtering on superalloys: a review', *Surface Engineering*, 41(2), pp. 149–175. doi: 10.1177/02670844251328622.

Ando, H., Ambe, Y., Ishii, A., Konyo, M., Tadakuma, K., Maruyama, S. and Tadokoro, S. (2018) 'Aerial hose type robot by water jet for fire fighting', *IEEE Robotics and Automation Letters*, 3(2), pp. 1128–1135. doi: 10.1109/LRA.2018.2792701.

Ariyanayagam, A. D. and Mahendran, M. (2014) 'Development of realistic design fire time–temperature curves for the testing of cold-formed steel wall systems', *Frontiers of Structural and Civil Engineering*, 8(4), pp. 427–447. doi: 10.1007/s11709-014-0279-1.

Bard, S., Schönl, F., Demleitner, M. and Altstädt, V. (2019) 'Influence of fiber volume content on thermal conductivity in transverse and fiber direction of carbon fiber-reinforced epoxy laminates', *Materials*, 12(7), p. 1084. doi: 10.3390/ma12071084.

Bellippady, M. et al. (2024) 'Performance of atmospheric plasma-sprayed thermal barrier coatings on additively manufactured super alloy substrates', *Coatings*, 14(5), p. 626. doi: 10.3390/coatings14050626.

Chen, D. and Dambra, C. (2024) 'Thick columnar-structured thermal barrier coatings using the suspension plasma spray process', *Coatings*, 14(8), p. 996. doi: 10.3390/coatings14080996.

Chen, X., Zhao, Y., Fan, X., Liu, Y., Zou, B., Wang, Y. et al. (2011) 'Thermal cycling failure of new $LaMgAl_{11}O_{19}$/YSZ double ceramic top coat thermal barrier coating systems', *Surface and Coatings Technology*, 205(10), pp. 3293–3300. doi: 10.1016/j.surfcoat.2010.11.059.

Cilento, F., Leone, C., Genna, S., Giordano, M. and Martone, A. (2023) 'Graphene NanoPlatelet-based coating as thermal protection from high-power radiative fluxes', *Composite Structures*, 319, p. 117157.

Clarke, D. and Levi, C. (2003) 'Materials design for the next generation thermal barrier coatings', *Annual Review of Materials Research*, 33(1), pp. 383–417. doi: 10.1146/annurev.matsci.33.011403.113718.

Clarke, D. R. and Phillpot, S. R. (2005) 'Thermal barrier coating materials', *Materials Today*, 8(6), pp. 22–29. doi: 10.1016/S1369-7021(05)70934-2.

Craig, M. et al. (2015) 'CMAS degradation of EB-PVD TBCs: the effect of basicity', *Surface and Coatings Technology*, 270, pp. 145–153. doi: 10.1016/j.surfcoat.2015.03.009.

Dai, S. et al. (2024) 'Cold spray technology and its application in the manufacturing of metal matrix composite materials with carbon-based reinforcements', *Coatings*, 14(7), p. 822. doi: 10.3390/coatings14070822.

Dennison, P. E., Charoensiri, K., Roberts, D. A., Peterson, S. H. and Green, R. O. (2006) 'Wildfire temperature and land cover modeling using hyperspectral data', *Remote Sensing of Environment*, 100(2), pp. 212–222. doi: 10.1016/j.rse.2005.10.007.

Dong, C., Li, K., Jiang, Y., Arola, D. and Zhang, D. (2018) 'Evaluation of thermal expansion coefficient of carbon fiber reinforced composites using electronic speckle interferometry', *Optics Express*, 26(1), pp. 531–543. doi: 10.1364/OE.26.000531.

Evans, A. G. et al. (2001) 'Mechanisms controlling the durability of thermal barrier coatings', *Progress in Materials Science*, 46(5), pp. 505–553. doi: 10.1016/S0079-6425(00)00020-7.

Fan, W. and Bai, Y. (2016) 'Review of suspension and solution precursor plasma sprayed thermal barrier coatings', *Ceramics International*, 42(13), pp. 14299–14312. doi: 10.1016/j.ceramint.2016.06.063.

Fang, Z., Li, M., Wang, S., Gu, Y., Li, Y. and Zhang, Z. (2019) 'Through-thickness thermal conductivity enhancement of carbon fiber composite laminate by filler network', *International Journal of Heat and Mass Transfer*, 137, pp. 1103–1111. doi: 10.1016/j.ijheatmasstransfer.2019.04.007.

International Journal of Health Sciences is licensed under a Creative Commons Attribution 4.0 International License

e-ISSN : 2987-0836 DOI: https://doi.org/10.59585/ijhs

Publish : Association of Indonesian Teachers and Lecturers
International Journal of Health Sciences (IJHS)
Journal Homepage : https://jurnal.agdosi.com/index.php/IJHS/index
Volume 4 | Number 4 | December 2026 |

Feuerstein, A., Knapp, J., Taylor, T., Ashary, A., Bolcavage, A. and Hitchman, N. (2008) 'Technical and economical aspects of current thermal barrier coating systems for gas turbine engines by thermal spray and EBPVD: a review', *Journal of Thermal Spray Technology*, 17(2), pp. 199–213. doi: 10.1007/s11666-007-9148-y.

Golewski, P. and Sadowski, T. (2018) 'A novel application of alumina fiber mats as TBC protection for CFRP/epoxy laminates – laboratory tests and numerical modeling', *Journal of the European Ceramic Society*, 38(8), pp. 2920–2927. doi: 10.1016/j.jeurceramsoc.2018.01.008.

Golewski, P. and Sadowski, T. (2019) 'Description of thermal protection against heat transfer of carbon fiber reinforced plastics (CFRP) coated by stiffened ceramic mat (TBC)', *Composite Structures*, 229, p. 111489. doi: 10.1016/j.compstruct.2019.111489.

Guo, D. et al. (2022) 'Cold spray: over 30 years of development toward a hot future', *Journal of Thermal Spray Technology*, 31(4), pp. 866–907. doi: 10.1007/s11666-022-01366-4.

He, Y.-L. and Xie, T. (2015) 'Advances of thermal conductivity models of nanoscale silica aerogel insulation material', *Applied Thermal Engineering*, 81, pp. 28–50. doi: 10.1016/j.applthermaleng.2015.02.013.

Hirata, Y., Itoh, S., Shimonosono, T. and Sameshima, S. (2016) 'Theoretical and experimental analyses of Young's modulus and thermal expansion coefficient of the alumina–mullite system', *Ceramics International*, 42(15), pp. 17067–17073. doi: 10.1016/j.ceramint.2016.07.216.

Hutchinson, J. W. and Evans, A. G. (2002) 'On the delamination of thermal barrier coatings in a thermal gradient', *Surface and Coatings Technology*, 149(2–3), pp. 179–184. doi: 10.1016/S0257-8972(01)01451-7.

Jarrah, M., Najafabadi, E. P., Khaneghahi, M. H. and Oskouei, A. V. (2018) 'The effect of elevated temperatures on the tensile performance of GFRP and CFRP sheets', *Construction and Building Materials*, 190, pp. 38–52. doi: 10.1016/j.conbuildmat.2018.09.086.

Ju, L., Yang, J., Hao, A., Daniel, J., Morales, J., Nguyen, S. et al. (2018) 'A hybrid ceramic-polymer composite fabricated by co-curing lay-up process for a strong bonding and enhanced transient thermal protection', *Ceramics International*, 44(10), pp. 11497–11504. doi: 10.1016/j.ceramint.2018.03.211.

Kandare, E., Khatibi, A. A., Yoo, S., Wang, R., Ma, J., Olivier, P. et al. (2015) 'Improving the through-thickness thermal and electrical conductivity of carbon fibre/epoxy laminates by exploiting synergy between graphene and silver nano-inclusions', *Composites Part A: Applied Science and Manufacturing*, 69, pp. 72–82. doi: 10.1016/j.compositesa.2014.10.024.

Khaneghahi, M. H., Najafabadi, E. P., Shoaei, P. and Oskouei, A. V. (2018) 'Effect of intumescent paint coating on mechanical properties of FRP bars at elevated temperature', *Polymer Testing*, 71, pp. 72–86. doi: 10.1016/j.polymertesting.2018.08.020.

Kim, H., Kim, J., Lee, J. and Lee, M. W. (2021) 'Thermal barrier coating for carbon fiber-reinforced composite materials', *Composites Part B: Engineering*, 225, p. 109308. doi: 10.1016/j.compositesb.2021.109308.

Kim, H., Praveen, K., Lee, M. W. and Lee, J. (2024) 'Performance-tunable thermal barrier coating for carbon fiber-reinforced plastic composites via flame spraying', *Composites Part B: Engineering*, 287, p. 111842. doi: 10.1016/j.compositesb.2024.111842.

Kim, Y., Ryu, K.-H., Na, W., Yu, J. and Lee, M. W. (2020) 'Origami-inspired reforming method for carbon fiber-reinforced thermoplastics via simple thermal stitching', *Composites Part B: Engineering*, 193, p. 108043. doi: 10.1016/j.compositesb.2020.108043.

Kodur, V. K. R., Bhatt, P. P. and Naser, M. Z. (2019) 'High temperature properties of fiber reinforced polymers and fire insulation for fire resistance modeling of strengthened concrete structures', *Composites Part B: Engineering*, 175, p. 107104. doi: 10.1016/j.compositesb.2019.107104.

Könnicke, D., Kühn, A., Mahrholz, T. and Sinapius, M. (2011) 'Polymer nanocomposites based on epoxy resin and ATH as a new flame retardant for CFRP: preparation and thermal characterisation', *Journal of Materials Science*, 46(21), pp. 7046–7055. doi: 10.1007/s10853-011-5673-7.

Krishnaswamy, S., Abhyankar, H., Marchante, V., Huang, Z. and Brighton, J. (2019) 'Aerogel/epoxy thermal coatings for carbon fibre reinforced plastic substrates', *Journal of Adhesion Science and Technology*, 33(6), pp. 579–594.

Lee, K. N., Fox, D. S., Eldridge, J. I., Zhu, D., Robinson, R. C., Bansal, N. P. and Miller, R. A. (2003) 'Upper temperature limit of environmental barrier coatings based on mullite and BSAS', *Journal of the American Ceramic Society*, 86(8), pp. 1299–1306. doi: 10.1111/j.1151-2916.2003.tb03466.x.

Leng, K., Romero, A. R. and Hussain, T. (2023) 'Multilayer GZ/YSZ thermal barrier coating from suspension and solution precursor thermal spray', *Journal of the European Ceramic Society*, 43(11), pp. 4991–5003. doi: 10.1016/j.jeurceramsoc.2023.04.014.

Liu, B., Liu, Y., Zhu, C., Xiang, H., Chen, H., Sun, L. et al. (2019) 'Advances on strategies for searching for next generation thermal barrier coating materials', *Journal of Materials Science & Technology*, 35(5), pp. 833–851. doi: 10.1016/j.jmst.2018.11.016.

International Journal of Health Sciences is licensed under a Creative Commons Attribution 4.0 International License

Publish : Association of Indonesian Teachers and Lecturers
International Journal of Health Sciences (IJHS)
Journal Homepage : https://jurnal.agdosi.com/index.php/IJHS/index
Volume 4 | Number 4 | December 2026 |

Liu, L. et al. (2024) 'Failure of electron beam physical vapor deposited thermal barrier coatings system under cyclic thermo-mechanical loading with a thermal gradient', *Coatings*, 14(7), p. 902. doi: 10.3390/coatings14070902.

Luangtriratana, P., Kandola, B. K. and Myler, P. (2015) 'Ceramic particulate thermal barrier surface coatings for glass fibre-reinforced epoxy composites', *Materials & Design*, 68, pp. 232–244. doi: 10.1016/j.matdes.2014.11.057.

Mehta, A. et al. (2022) 'Processing and advancements in the development of thermal barrier coatings: a review', *Coatings*, 12(9), p. 1318. doi: 10.3390/coatings12091318.

Mittal, G. and Paul, S. (2022) 'Suspension and solution precursor plasma and HVOF spray: a review', *Journal of Thermal Spray Technology*, 31(5), pp. 1443–1475. doi: 10.1007/s11666-022-01360-w.

Moridi, A., Azadi, M. and Farrahi, G. H. (2014) 'Thermo-mechanical stress analysis of thermal barrier coating system considering thickness and roughness effects', *Surface and Coatings Technology*, 243, pp. 91–99. doi: 10.1016/j.surfcoat.2012.02.019.

Morvan, D. and Dupuy, J.-L. (2004) 'Modeling the propagation of a wildfire through a Mediterranean shrub using a multiphase formulation', *Combustion and Flame*, 138(3), pp. 199–210. doi: 10.1016/j.combustflame.2004.05.001.

Nguyen, P. L., Vu, X. H. and Ferrier, E. (2019) 'Thermo-mechanical performance of carbon fiber reinforced polymer (CFRP), with and without fire protection material, under combined elevated temperature and mechanical loading conditions', *Composites Part B: Engineering*, 169, pp. 164–173. doi: 10.1016/j.compositesb.2019.03.075.

Nieto, A. et al. (2021) 'Calcia–magnesia–alumina–silicate (CMAS) attack mechanisms and roadmap towards sandphobic thermal and environmental barrier coatings', *International Materials Reviews*, 66(7), pp. 451–492. doi: 10.1080/09506608.2020.1824414.

Padture, N. P., Gell, M. and Jordan, E. H. (2002) 'Thermal barrier coatings for gas-turbine engine applications', *Science*, 296(5566), pp. 280–284. doi: 10.1126/science.1068609.

Peng, H. et al. (2012) 'Degradation of EB-PVD thermal barrier coatings caused by CMAS deposits', *Progress in Natural Science: Materials International*, 22(5), pp. 461–467. doi: 10.1016/j.pnsc.2012.06.007.

Praveen, K., Kim, H., Lee, J., Cha, J.-H. and Lee, M. W. (2026) 'High-performance ceramic thermal barrier coatings for carbon fiber-reinforced plastics developed by atmospheric plasma spraying', *Composites Part A: Applied Science and Manufacturing*, 201, p. 109424. doi: 10.1016/j.compositesa.2025.109424.

Restas, A. (2015) 'Drone applications for supporting disaster management', *World Journal of Engineering and Technology*, 3(3), pp. 316–321. doi: 10.4236/wjet.2015.33C047.

Soleimanipour, Z., Baghshahi, S., Shoja-Razavi, R. and Salehi, M. (2016) 'Hot corrosion behavior of Al_2O_3 laser clad plasma sprayed YSZ thermal barrier coatings', *Ceramics International*, 42(15), pp. 17698–17705. doi: 10.1016/j.ceramint.2016.08.090.

Tejero-Martin, D. et al. (2019) 'Beyond traditional coatings: a review on thermal-sprayed functional and smart coatings', *Journal of Thermal Spray Technology*, 28, pp. 598–644. doi: 10.1007/s11666-019-00857-1.

Tian, T. and Cole, K. D. (2012) 'Anisotropic thermal conductivity measurement of carbon-fiber/epoxy composite materials', *International Journal of Heat and Mass Transfer*, 55(23–24), pp. 6530–6537. doi: 10.1016/j.ijheatmasstransfer.2012.06.059.

Vaßen, R. et al. (2010) 'Overview on advanced thermal barrier coatings', *Surface and Coatings Technology*, 205(4), pp. 938–942. doi: 10.1016/j.surfcoat.2010.08.151.

Wang, L. et al. (2022) 'Effects of TGO growth on the stress distribution and evolution of three-dimensional cylindrical thermal barrier coatings based on finite element simulations', *Ceramics International*, 48(6), pp. 7864–7875. doi: 10.1016/j.ceramint.2021.11.334.

Xie, L. et al. (2004) 'Processing parameter effects on solution precursor plasma spray process spray patterns', *Surface and Coatings Technology*, 183(1), pp. 51–61. doi: 10.1016/j.surfcoat.2003.09.071.

Yao, Y., Yang, F. and Zhao, X. (2022) 'Multicomponent high-entropy Zr-Y-Yb-Ta-Nb-O oxides for next-generation thermal barrier coating applications', *Journal of the American Ceramic Society*, 105(1), pp. 35–43. doi: 10.1111/jace.18053.

Ye, D. et al. (2024) 'Terahertz non-destructive testing of porosity in multi-layer thermal barrier coatings based on small-sample data', *Coatings*, 14(11), p. 1357. doi: 10.3390/coatings14111357.

Yu, G.-C., Wu, L.-Z. and Feng, L.-J. (2015) 'Enhancing the thermal conductivity of carbon fiber reinforced polymer composite laminates by coating highly oriented graphite films', *Materials & Design*, 88, pp. 1063–1070. doi: 10.1016/j.matdes.2015.09.096.

Zhao, D. et al. (2024) 'Melt-grown behaviour of heat treated high-purity alumina ceramics prepared by laser directed energy deposition', *Ceramics International*, 50(1), pp. 1777–1787. doi: 10.1016/j.ceramint.2023.10.277.

Zhao, D. et al. (2025) 'Thermal properties for Al_2O_3-based melt-grown ceramics prepared by laser-directed energy deposition', *Journal of Alloys and Compounds*, 1010, p. 177795. doi: 10.1016/j.jallcom.2024.177795.

Zhou, D. et al. (2024) 'Microstructure and thermal shock behavior of CoMoCrSi coatings prepared by HVOF and APS', *Surface and Coatings Technology*, 478, p. 130498. doi: 10.1016/j.surfcoat.2024.130498.

International Journal of Health Sciences is licensed under a Creative Commons Attribution 4.0 International License

e-ISSN : 2987-0836 DOI: https://doi.org/10.59585/ijhs

Publish : Association of Indonesian Teachers and Lecturers
International Journal of Health Sciences (IJHS)
Journal Homepage : https://jurnal.agdosi.com/index.php/IJHS/index
Volume 4 | Number 4 | December 2026 |

Zhu, D. and Miller, R. A. (2000) 'Thermal-barrier coatings for advanced gas-turbine engines', *MRS Bulletin*, 25(7), pp. 43–47. doi: 10.1557/mrs2000.123.

Zhu, H. et al. (2023) 'Prediction of microstructure and mechanical properties of atmospheric plasma-sprayed 8YSZ thermal barrier coatings using hybrid machine learning approaches', *Coatings*, 13(3), p. 602. doi: 10.3390/coatings13030602.

International Journal of Health Sciences is licensed under a Creative Commons Attribution 4.0 International License